Formation and Decay Behaviors of Laser-Induced Transient Species from Pyrene Derivatives 1. Spectral Discrimination and Decay Mechanisms in Aqueous Solution

Yoshihiro Mori,* Hiroyuki Shinoda, Taku Nakano, and Taiji Kitagawa

Department of Pharmaceutical Sciences, Toyama Medical and Pharmaceutical University, Sugitani, Toyama 9300194, Japan

Received: February 5, 2002; In Final Form: August 16, 2002

The ultraviolet and visible absorption spectra of laser-induced transient species from the following pyrene derivatives were measured in aqueous or aqueous ethanol solution: sodium pyrenesulfonate (NaPS), tetrasodium pyrenetetrasulfonate (Na_4PS_4), pyrenecarboxylic acid (HPC), and pyrenebutyric acid (HPB). The major transient species contributing to the intense absorption peaks were revealed on the basis of the quenching experiments. The absorption spectra of triplets, as well as cation radicals, were separable from the other transients by selecting the experimental conditions (atmosphere, coexisting quencher, and delay time). The cation radicals produced from PS^-, PB^- and PC^- anions showed an absorption maximum at ∼460 nm, close to that of pyrene cation radical. Their decay behaviors in the absence of any additional quenchers were dominated by bimolecular reaction kinetics with each parent molecule, of which the rate constants were very similar. This result is consistent with the previous proposal that these cation radicals exist as zwitterions such as $P^{\bullet+}S^-$. The cation radical from Na_4PS_4 showed a strong absorption peak at 505 nm and exhibited different decay behaviors, suggesting that this cation radical appears not to be a simple zwitterion. Three specific quenchers, I^-, OH^-, and SO_3^{2-}, were found to strongly accelerate the decay rates of these cation radicals. $CH_3SO_3^-$ anion, mimicking the headgroup of tentative anionic surfactants, and several inorganic anions such as ClO_4^- were poor quenchers for the cation radicals even at the highest concentration. We also discussed the origin of two additional peaks at 375 and 395 nm observed in the transient absorption spectra of NaPS and HPB. On the triplet−triplet absorption, the molar extinction coefficients of Na_4PS_4 and NaPS could be determined using the ground-state depletion method. These results are discussed in terms of applications to probe the micellar microenvironment.

Introduction

Pyrene and its numerous derivatives have been widely used to probe the microscopic environment and the dynamic behavior in molecular aggregated systems such as micelles or microemulsions.[1,2] Their excellent probing abilities are greatly due to the photophysical and photochemical properties involving fluorescence and formation of excited complexes. The fluorescence spectra of most pyrene derivatives are very similar to that of pyrene. The transition probability from the ground state (S0) to the lowest singlet excited state (S1) of pyrene is so small (nominally forbidden) that the fluorescence spectrum is observed via the excitation to the second singlet excited state (S2). The observed fluorescence, however, is very strong and assignable to the transition from S1 to S0. Such an enhanced fluorescence can be explained by the vibronic coupling between S1 and S2, involving the solute−solvent interaction associated with the nuclear displacement along the special vibrational coordinate.[3] This interaction is known to induce a strong dependence of the fluorescence intensity of the first vibronic band (I_1) on solvent polarity. Thus, the relative intensity of I_1/I_3 has successfully been employed as a micropolarity scale of the environment surrounding the probe,[1−6] where I_3 is the intensity of the third vibronic band, which is less sensitive to the solvent polarity. A similar scale was also examined in several pyrene derivatives such as pyrenesulfonate, which showed a strong S0−S2 absorption and a very weak S0−S1 absorption.[7,8] The fluorescences of pyrene and its derivatives have significantly long lifetimes ranging from a few tens to a few hundreds of nanoseconds, which are comparable to or longer than the time-scale for diffusion of a probe within a micelle and collision between micelles. This makes it possible to observe excimer fluorescence and intermicellar quenching behavior. From those findings, the aggregation number of surfactants and the microviscosity within a micelle can be deduced.[9−13]

When a high power UV laser is used as an exciting light source, the two-photon ionization process occurs in pyrene and its derivatives, leading to the formation of cation radicals, solvated electrons, and anion radicals and then induction of photochemical reactions. These transient species involving triplets generated via the one-photon process, which are detectable with transient absorption (TA) spectroscopy, have also been employed as a probe to investigate the microscopic environment in micellar systems. In early studies, Grätzel et al. suggested that the micellar Stern layer, in addition to the location of the probe, plays an important role in the photoionization process of several pyrene derivatives.[14] Since then, several studies have revealed that the size of the water pool strongly affects the two-photon ionization[15−17] and triplet annihilation.[18] This method, however, has rarely been applied in this decade, while the fluorescence method has become increasingly more common to investigate the properties of micellar systems.[19−22] This may be caused mainly by the lack of knowledge on the detailed decay mechanism for these transient species and the difficulty to separate individual spectra.

10.1021/jp020332l CCC: $22.00 © 2002 American Chemical Society
Published on Web 11/13/2002

The decay behaviors of triplets (T) have been extensively investigated. The results show that the triplets decay dominantly through the T−T annihilation (TTA) mechanisms. Rothenberger et al. successfully analyzed the TTA process in CTAB micellar systems containing 1-bromonaphthalene as a probe molecule (CTAB; cetyltrimethylammonium bromide).[18] However, the detailed mechanism of TTA, in addition to the reliable extinction coefficients for the T−T absorption peaks, has not been revealed for most pyrene derivatives. Furthermore, the decay behaviors of the cation and anion radicals from pyrene derivatives have remained uncertain or untouched. The spectral overlap is inevitable when a high power laser is employed because various kinds of transient species coexist. The spectral discrimination of these transient species may in principle be possible because specific quenchers for triplet, cation, and anion radicals are known, that is, O_2, I^-, and N_2O, respectively.

Here, we examined or reexamined in detail the TA spectra of the following four pyrene derivatives in aqueous or aqueous ethanol solution from these points of view: sodium 1-pyrenesulfonate (NaPS), tetrasodium 1,3,6,8-pyrenetetrasulfonate (Na_4PS_4), 1-pyrenecarboxylic acid (HPC), and 1-pyrenebutyric acid (HPB). The observed TA spectra involved several characteristic peaks. Most were previously detected, but their assignment in part remains confused. A few have not been detected or attracted no attention in previous studies. So, we systematically investigated the dependence of the peak intensity and the decay behavior on atmospheric gas (Ar, N_2, N_2O, or O_2), laser power, and the presence of a quencher such as I^-. This dependence made it possible to assign the TA peaks unequivocally and obtain nearly pure spectral shapes of the cation radical and the triplet. The quenching behaviors of transient species have been observed in the presence of various kinds of inorganic and organic salts in as high concentrations as possible to mimic a micellar environment. In another paper, we will present the micellar effects on the formation and decay behaviors of those transient species and discuss their application to probe the microscopic environment of micellar systems.

Experimental Section

TA Measurements. TA spectra and the decay behavior were measured using the modified apparatus reported previously.[16] The excitation was performed mainly with the third harmonics (355 nm) of a Nd:YAG laser unfocused at about 4 mJ/8 mm^2 (50 mJ/cm^2) and partly with a XeF excimer laser (351 nm) focused at 3−4 mJ/6 mm^2 (50−65 mJ/cm^2). The short arc Xe lamp was used as the monitor light source. The signal at each wavelength, detected with the photomultiplier, was stored on the digital oscilloscope and transferred to a personal computer. The observed temporal range after laser irradiation was covered from 0 to 10−90 μs at 5−50 ns per point. Each signal was averaged for 10−20 shots of laser irradiation.

The measurements of molar extinction coefficients for T−T absorption were carried out by the ground-state depletion method.[23−25] The laser light (Nd:YAG, 355 nm) was irradiated on the rectangular area of the cell (1 cm of width and 0.5 cm of height). The laser pulse energy was maintained at about 3 mJ/cm^2.

Materials and Sample Preparation. All of the pyrene derivatives used in this study were purchased from Molecular Probe Inc. and used without further purification. Inorganic and organic salts, as commercially available quenchers, were used as received. Sodium methylsulfonate was prepared by neutralizing methylsulfonic acid with aqueous NaOH solution. Doubly distilled water and ethanol (spectral grade) were used as solvents.

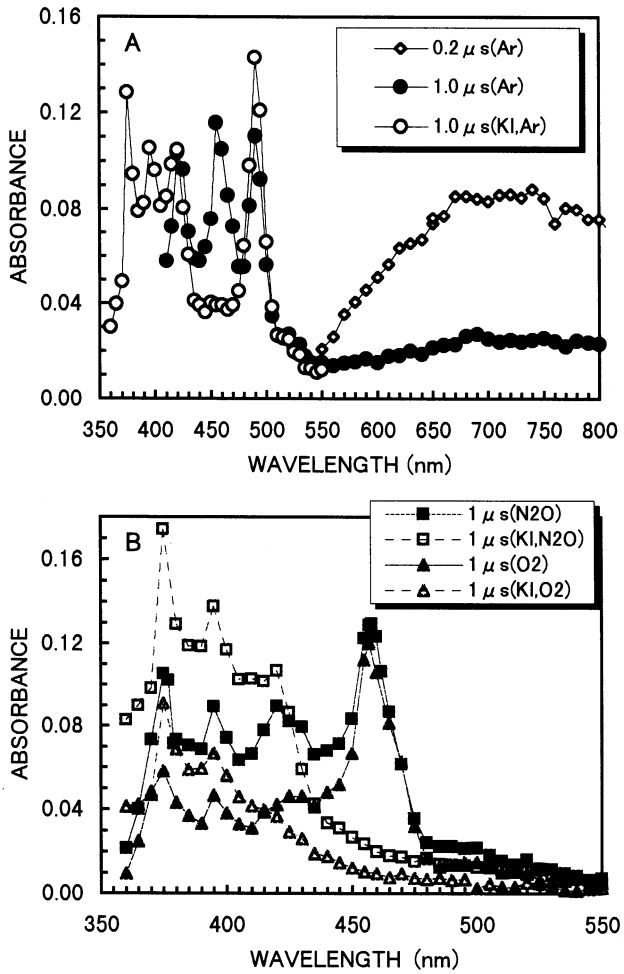

Figure 1. The TA spectra of NaPS in an aqueous solution (1.0×10^{-4} M) containing 0 (filled symbols) and 8×10^{-4} M (empty symbols) KI: (A) the TA spectra observed under Ar. The absorbance data at 1 μs in the wavelength range shorter than 405 nm were eliminated because of the overlap of the strong fluorescence signal from NaPS under Ar. Panel B shows the TA spectra observed under N_2O and O_2.

The aqueous or aqueous ethanol solution containing a probe molecule (usually 1×10^{-4} M (M = mol/dm^3)) and a quencher was prepared and deaerated by several freeze−pump−thaw cycles and saturated with high-purity gas of Ar, N_2, O_2, or N_2O. The solution was maintained at 25 ± 0.5 °C using a water circulator. Because a significant amount of the probe molecules were photochemically decomposed after the long exposure of the high-power laser, the sample solution was stirred during measurement and frequently exchanged for a fresh solution (typically after exposure to about 50 shots). For example, 10% of Na_4PS_4 molecules in aqueous solution (the initial concentration of 2×10^{-5} M) were converted to pyranine after irradiating for about 30 shots under N_2O. This is the situation in which the photodecomposition proceeds most rapidly.

Results and Discussion

1. Overview of TA Spectra. *NaPS.* Figure 1A shows the TA spectra of NaPS in aqueous solution observed under Ar. Four major peaks were observed at 420, 457, 700−750, and 490 nm. The former three peaks have been assigned to the absorptions of triplets (T−T), cation radicals, and hydrated electrons, respectively.[14,16,26−30]

The 490 nm peak can very likely be assigned to the anion radical,[16,27,31] but some different assignments have been pro-

posed.[26,29,30,32] Here, we could unequivocally attribute this peak to the anion radical on the basis of the finding that this absorption rapidly disappeared in the presence of N_2O, an effective quencher of electrons,[33] as shown in Figure 1B. Other evidence was reported previously that this transient was generated via a two-photon process and attained its maximum absorbance approximately 1 μs after laser irradiation,[16,27,28] which also supports this assignment. These results suggest that the anion radical is a dianion, $P^{\bullet-}S^-$, formed via attachment of photoejected electron to PS^-.

The assignment of the 457 nm peak to the cation radical was confirmed on the basis of the experimental results that the peak was rapidly quenched by I^-, an effective quencher of cation radicals, and was only slightly affected by N_2O and O_2. The TA spectrum observed at 1 μs under O_2, shown as filled triangles in Figure 1B, exhibited four peaks at 375, 395, 425−430, and 495−500 nm, in addition to the strong peak at 457 nm. The latter two weak peaks were assigned to the cation radical on the basis of their efficient quenching by I^-. The former two peaks at 375 and 395 nm, however, were not attributable to the cation radical. They showed unusual quenching behaviors by I^-. When KI was added to the solution, the absorbance in the wavelength range from 360 to 405 nm increased by about 50% under O_2 and N_2O as shown in Figure 1B. Such a marked enhancing effect was not detected by adding other inorganic salts such as KCl, KF, NaBr, Na_2SO_3, Na_2SO_4, NaOH, or $NaNO_3$. Furthermore, the absorbance significantly increased under N_2O. Thus, the quenching experiments suggest that the transient species detected in this wavelength range are neither triplet nor the two ionic radicals (cation and anion).

The spectral shape in this wavelength range (peak position and relative intensity) was very similar to the fluorescence spectrum of NaPS in aqueous solution. However, the TA could be detected even in the temporal range far beyond the fluorescence lifetime. The absorbance at 375 nm ($A(t)$) was described by the following biexponential decay function: $A(t) = A_1 \exp(-t/\tau_1) + A_2 \exp(-t/\tau_2)$. The lifetimes of τ_1 and τ_2 were estimated to be 1.3−1.9 and 18−25 μs, respectively, depending on the experimental conditions. The coefficients A_1 and A_2 obtained with the absorbance data observed under N_2O showed different dependence on both laser pulse energy and I^-. At the range lower than 2 mJ, both A_1 and τ_1 (1.4 ± 0.1 μs) were little changed by adding KI. The exponents obtained in this range of laser pulse energy were nearly equal to that for T−T absorption observed at 420 nm, suggesting that this species with a short lifetime was formed via the one-photon process. The coefficient A_2 for slowly decaying species steeply increased with laser pulse energy. The dependence was similar to that of the absorbance at 460 nm mainly attributable to the $P^{\bullet+}S^-$ cation radical, suggesting that this species was generated via the two-photon process. The values of A_2 increased by about 50% when KI was added. On the basis of these experimental findings, it is suggested that the transient absorption at 375 nm was due mainly to the following two possible intermediate species: $(PS^-)^‡$ and $(I_2)^{\bullet-}$. $(PS^-)^‡$ is the unrelaxed species immediately after the fluorescence is emitted from the S1 excited state. This transient species mainly contributes to A_1. The lowest and the second singlet excited states S1 and S2 of pyrene and some pyrene derivatives are known to interact strongly through solvent molecules. This interaction can induce a strong fluorescence from S1 although the absorption cross-section for the transition from S0 to S1 is very small. Therefore, $(PS^-)^‡$ is considered to retain the interactive structure of the S1 state and to slowly relax into the ground state of PS^-. If so, $(PS^-)^‡$ could efficiently re-

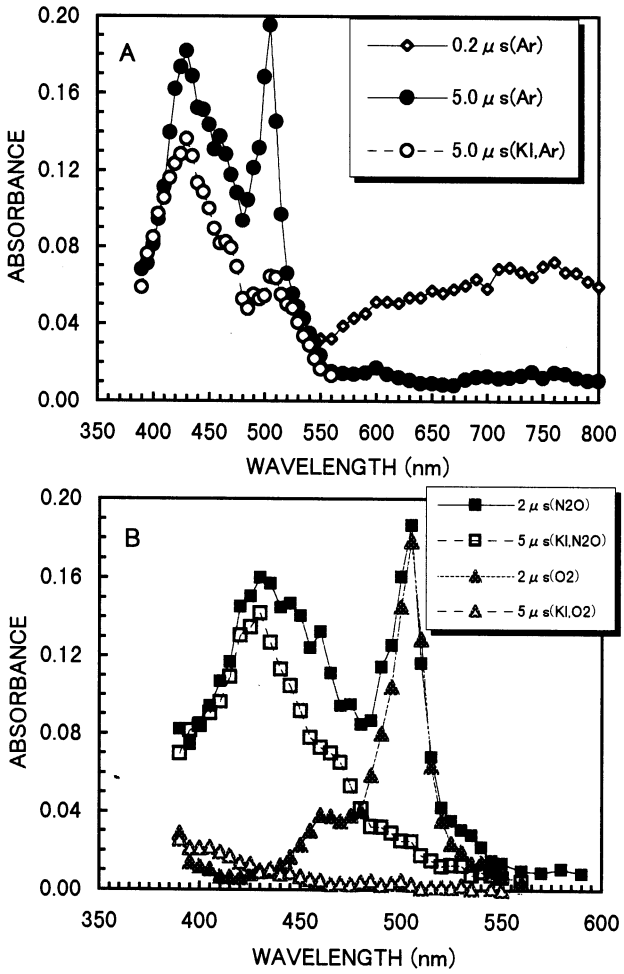

Figure 2. The TA spectra of Na_4PS_4 in an aqueous solution (1.3×10^{-4} M) containing 0 (filled symbols) and 1.1×10^{-3} M (empty symbols) KI: (A) the TA spectra observed under Ar; (B) the TA spectra observed under N_2O and O_2.

absorb the monitor light at the same wavelength as that of the fluorescence peak. $(I_2)^{\bullet-}$ is known to be an intermediate species formed in the quenching reaction of the cation radical with I^-.[30] This species was suggested to dominantly contribute to A_2 because the corresponding transient species was formed via the two-photon process and enhanced by I^-. This assignment is also supported by the previous results that the $(I_2)^{\bullet-}$ anion radical shows a broad spectrum around 370 nm with a long lifetime.[34]

Na_4PS_4. The TA spectra of the Na_4PS_4 solution under Ar shown in Figure 2A involve two strong peaks at 430 and 505 nm and a shoulder-like peak at 460 nm. The two peaks at 430 and 505 nm have been assigned to the T−T absorption and the cation radical, respectively.[29] These assignments were confirmed with the quenching experiments using O_2 and I^-, respectively. A significant amount of hydrated electrons were also observed as a broad TA peak at 700−750 nm. Nevertheless, the anionic radical of PS_4^{4-} was not detected as an explicit TA peak as that of $P^{\bullet-}S^-$. If no anionic radicals were formed, the absorbance around 505 nm should be similar under N_2O and Ar. However, the absorbance observed under Ar was significantly larger than that under N_2O. This was explicitly shown by comparing the TA spectra observed in the presence of the I^- anion under Ar and N_2O. The difference spectrum showed a weak maximum at ca. 510 nm. This result suggests that a small amount of the anion radicals contribute to the TA spectra in this wavelength range.

The TA spectra of the triplet and the cation radical can be separated from each other as follows. The former is given by the TA spectrum observed at 5 μs in aqueous solution containing KI under N_2O (empty squares in Figure 2B), in which both the anion and the cation radicals are completely quenched. From this spectrum, the contribution of T−T absorption to the peak at 505 nm was found to be significantly large. On the other hand, the absorption spectrum of the cation radical is given by the TA spectrum observed at a sufficiently long delay time under O_2 in which both the triplet and the anion radical are quenched. This spectrum involves a shoulder-like peak at 460 nm, in addition to the main peak at 505 nm. The perturbation of the cation radical to the T−T absorption maximum at 430 nm was found to be negligibly small.

The TA spectra of trisodium 1-acetoxy-3,6,8-pyrenetrisulfonate (Na_3APS_3) observed under Ar were very similar to those of Na_4PS_4, which showed the two absorption peaks at 430 and 505 nm attributable to the absorptions of T−T and cation radical, respectively.

HPB and HPC. Because HPB and HPC were sparsely dissolved in water, their TA spectra were measured in aqueous ethanol solution (1:1 v/v). TA spectra of HPB were similar to those of NaPS. The observed peaks at 415, 460, 495, and 700−750 nm were assigned to be T−T, cation radical, anion radical, and solvated electron, respectively. These assignments were consistent with the previous results.[14,30] The spectrum of the cation radical separated from the other transients such as the triplet and the anion radical was found to give two weak peaks at 430 and 490−495 nm, in addition to the main peak at 460 nm. TA spectrum that was enhanced by I^- like the fluorescence spectrum was also observed at the wavelengths shorter than 400 nm. In the case of HPC, the absorption peaks attributable to the T−T absorption and the anion radical were detected at 430 and 495 nm, respectively. The cation radical gave a strong peak at 460 nm and two shoulders at 435−440 and 495−500 nm.

2. Decay of Cation Radicals. *Decay Mechanism in the Absence of an Additional Quencher.* The cation radicals from NaPS, HPB, and HPC commonly give a strong TA peak at 455−460 nm, approximately equal to that of the pyrene cation radical (450 nm).[30,35] These peaks involved significant contributions from several transients other than the cation radical: triplet, anion radical, and unknown species. The former two could be eliminated by analyzing the TA signals in the temporal range of microseconds observed under O_2 because they were completely quenched within a few hundred nanoseconds. The third transients were minor species and had a very long lifetime, so they could be eliminated as a constant value. Thus, the decay curves observed at 460 nm under O_2 were analyzed using the following decay function: $A(t) = A_0 \exp(-kt) + A_1$; $A(t)$ is the observed absorbance at time t (s) after laser irradiation; k is the decay constant (s^{-1}); A_0 and A_1 are constants. Typical examples of the decay curves and the fitting curves in the case of NaPS are shown in Supporting Information (Figure 1S). The observed decay curves were found to greatly depend on the initial concentration of the probe molecule. The decay constants linearly increased with the molar concentration of NaPS ([NaPS]) as shown in Figure 3: k_{PS} (s^{-1}) = (5.5 ± 0.1) × 10^9[NaPS] + (7 ± 2) × 10^4. The decay constants were independent of the initial concentration of the cation radical, that is, laser power. This means that the cation radical−cation radical annihilation[30] does not contribute to the quenching of the cation radical. The dominant decay mechanism, therefore,

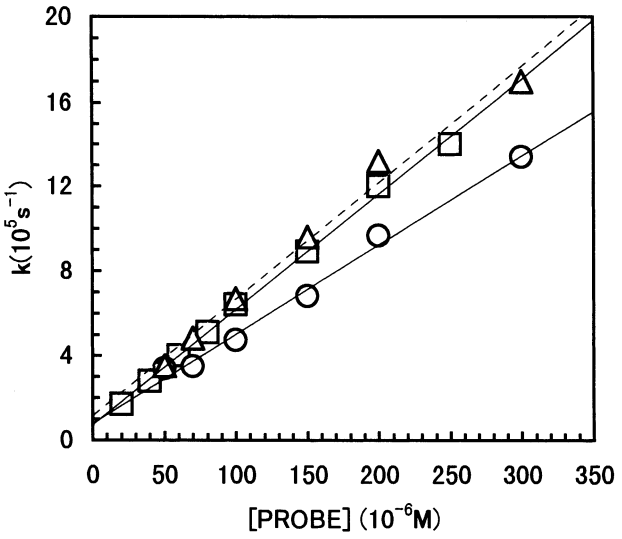

Figure 3. Dependence of decay constants of a cation radical (k) on [probe]: (□) $(PS^-)^{\bullet+}$; (△) $(PC^-)^{\bullet+}$ (0.1 M NaOH); (○) $(PB^-)^{\bullet+}$ (0.1 M NaOH). One broken and two solid lines were calculated using the least-squares fitting method. The errors of k at a given [probe] were estimated to be ≤5% (see Supporting Information (caption of Figure 1S)).

is presented by the following bimolecular reaction:

$$(PS^-)^{\bullet+} + PS^- \rightarrow \text{products}$$

A similar bimolecular quenching reaction was found to be dominant in the decay behaviors of HPB and HPC cation radicals observed in the 0.1 M NaOH solution, in which HPB and HPC existed as pyrene butyrate (PB^-) and pyrene carboxylate (PC^-) anions, respectively. The rate constants were nearly equal to that of PS^- cation radical: k_{PB} (s^{-1}) = (4.2 ± 0.2) × 10^9[PB^-] + (8 ± 3) × 10^4; k_{PC} (s^{-1}) = (5.5 ± 0.3) × 10^9[PC^-] + (12 ± 5) × 10^4. These relations are shown in Figure 3. Such similarities of the decay kinetics, in addition to the absorption peaks, suggest that these cation radicals exist as zwitterions involving a common pyrenyl cation radical, that is, $P^{\bullet+}S^-$, $P^{\bullet+}B^-$, or $P^{\bullet+}C^-$. The results of MO calculations for the PS^- + H_2O systems also supported this zwitterion model: the first ionization state of PS^- is formed via the ionization of π-electron delocalized on the pyrenyl frame.[36]

The cation radical from PS_4^{4-} was found to decay very slowly with lifetimes of 0.7 ms under Ar and 0.4 ms under N_2O. The lifetime under O_2, however, was markedly shortened to be about 50 μs. The decay rates did not show any significant dependence on [PS_4^{4-}] (≤3 × 10^{-4} M). Hence, this cation radical appears not to be a simple zwitterion such as $P^{\bullet+}S_4^{4-}$. A marked micellar effect on this transient will be reported in the second paper, which should provide an answer to the question.

Quenching by Several Anions. In this section, we investigated the quenching behaviors of the cation radicals in the presence of the following anions: I^-, OH^-, SO_3^{2-}, $CH_3SO_3^-$, SO_4^{2-}, ClO_4^-, Cl^-, Br^-, and F^-.

(1) I^- Anion. The I^- anion is one of the most effective quenchers of cation radicals. The decay curves of the cation radicals were measured under O_2 in the presence of I^- ($0 \le [I^-] \le 5 \times 10^{-4}$ M). The decay constants were determined as a function of [I^-] with the same fitting method used for the decay analysis of the cation radicals in the absence of I^-. The $P^{\bullet+}S^-$ cation radical was most rapidly quenched by I^-, of which lifetime was only 0.15 μs when [KI] = 8 × 10^{-4} M and [NaPS] = 1 × 10^{-4} M. The decay constant of $P^{\bullet+}S^-$ ((7.9 ± 0.3) × 10^9 M^{-1} s^{-1}), in agreement with the reported value (7.86 ×

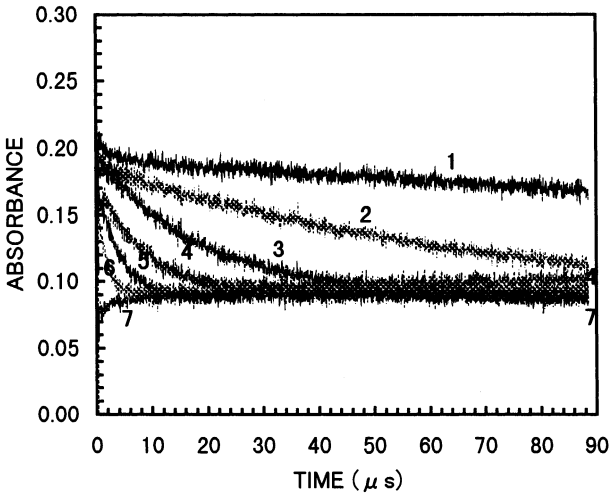

Figure 4. Quenching behavior of the $(PS_4^{4-})^{\bullet+}$ cation radical by OH^- anion as a function of [NaOH]. The numbers 1−7 show the decay curves for the PS_4^{4-} solution containing 0, 0.03, 0.05, 0.10, 0.20, and 0.50 M NaOH, respectively. The decay curves were observed at 505 nm under N_2.

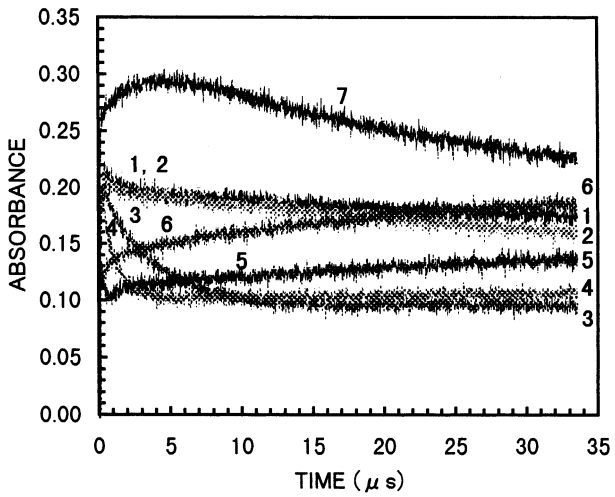

Figure 5. Quenching behavior of the $(PS_4^{4-})^{\bullet+}$ cation radical by the SO_3^{2-} anion as a function of [Na_2SO_3]. The numbers 1−7 show the decay curves for the PS_4^{4-} solution containing 0, 0.005, 0.010, 0.020, 0.050, 0.10, and 0.40 M of Na_2SO_3, respectively. The decay curves were observed at 505 nm under N_2.

10^9 M^{-1} s^{-1}),[30] was 8.1- and 4.4-fold greater than those of the cation radicals from PS_4^{4-} and APS_3^{3-}, respectively. This difference may be explained by a strong electrostatic repulsive interaction between the I^- anion and the cation radicals of $(PS_4^{4-})^{\bullet+}$ and $(APS_3^{3-})^{\bullet+}$, of which net charges are negative.

(2) OH^- Anion. In an alkaline solution containing NaOH, the cation radical of PS_4^{4-} rapidly decayed with an increase in [NaOH] as shown in Figure 4. The observed TA at 505 nm involved several transient species other than the cation radical. The main contributor was the T−T absorption as described above, which was estimated to be about 0.03−0.04 in absorbance units and nearly constant in the temporal range investigated. Therefore, the characteristic decay behaviors depending on [NaOH] were mainly due to the cation radical, $(PS_4^{4-})^{\bullet+}$. It was shown that the decay rates acceleratedly increased with [NaOH] below 0.2 M. With a further increase in [NaOH], the decay was too fast to detect and then the absorbance gradually increased, suggesting that a new product was generated. We are now investigating the relation between this product and the formation of the final photoproduct, that is, pyranine (see Experimental Section). The $P^{\bullet+}S^-$ cation radical was also quenched by OH^-, but the quenching rate was much slower than those of $(PS_4^{4-})^{\bullet+}$. The lifetime of the $P^{\bullet+}S^-$ cation radical in 1 M NaOH was 0.5 μs in comparison with 1.3 μs observed in pure water under O_2. The other transients such as triplet and anion radicals were only affected a little by OH^-.

(3) SO_3^{2-} Anion. This anion showed unusual quenching behavior for the cation radical of PS_4^{4-}. Figure 5 shows the decay behavior as a function of [SO_3^{2-}]. In the concentration range lower than 0.02 M, the cation radical decayed as rapidly as in the same concentration range of [NaOH]. However, above 0.05 M, this cation radical very rapidly decayed to form a new species accompanied with an increase in the absorbance. At 0.40 M, the absorbance reached the maximum at about 4 μs after laser irradiation, of which the absorbance was larger than that observed in pure PS_4^{4-} aqueous solution. Figure 6 shows the TA spectra of Na_4PS_4 in 0.40 M Na_2SO_3 solution. Two peaks at 510 and 600 nm appeared instead of the peak at 505 nm. We can suppose some transient species contributing to these TA peaks. One possible transient is that formed during the recombination reaction between SO_3^{2-} anion and an intermediate in the photodesulfonation in aqueous solution of PS_4^{4-}. The

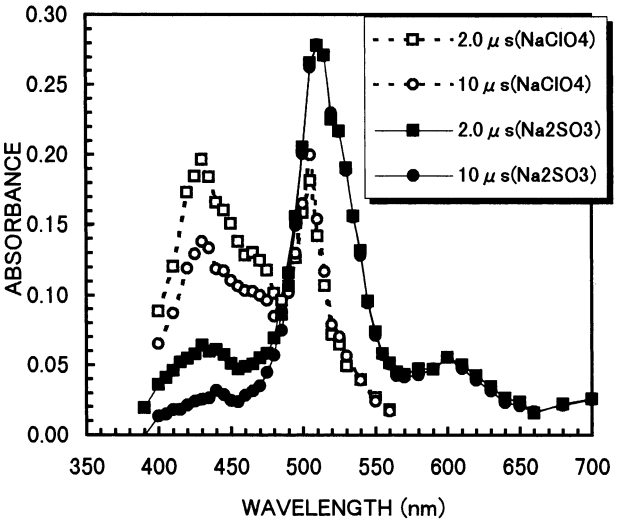

Figure 6. The TA spectra of Na_4PS_4 in 0.4 M Na_2SO_3 (filled symbols) and 4 M $NaClO_4$ (empty symbols) solutions under N_2.

latter intermediate, in the absence of SO_3^{2-} anion, could react with OH^- or H_2O to yield pyranine. The $P^{\bullet+}S^-$ cation radical was also quenched by SO_3^{2-} with the rate constant of $(2.4 \pm 0.2) \times 10^9$ M^{-1} s^{-1}. The other transients were not significantly affected in the presence of SO_3^{2-}, and no new TA peaks appeared.

(4) $CH_3SO_3^-$ and Other Anions. The $CH_3SO_3^-$ anion, as a model anionic species to mimic the headgroup of typical anionic surfactant (AOT), was found to be a very poor quencher for the cation radicals. The ClO_4^-, SO_4^{2-}, F^-, and Cl^- anions also showed only a small effect on the decay rate of the $(PS_4^{4-})^{\bullet+}$ cation radical (see Supporting Information). The TA spectra of PS_4^{4-} observed in highly ionic solutions involving these anions, for example, in 4 M $NaClO_4$, were similar to the TA spectrum in aqueous solution as shown in Figure 6.

3. T−T Absorption. Most of the pyrene derivatives investigated showed the T−T absorption at 415−430 nm, close to that of pyrene (415−420 nm).[30,34,35] The decay rates of the monosubstituted pyrenes (PS^- and HPB) were significantly faster than those of PS_4^{4-} and APS_3^{3-}. Oxygen gas was the most effective quencher for the T−T absorption, while most of

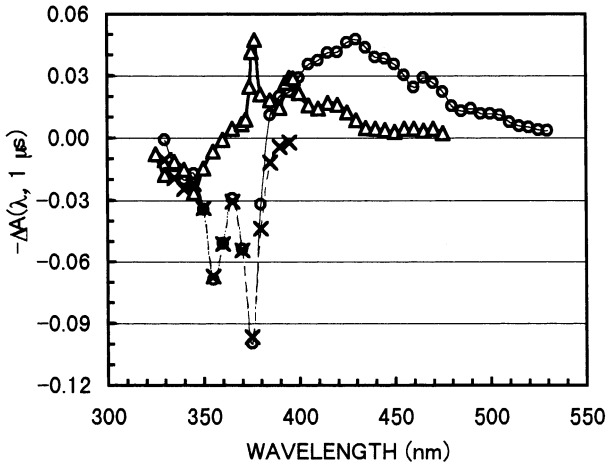

Figure 7. Difference spectra ($-\Delta A(\lambda,1\ \mu s)$) of Na_4PS_4 (○) and NaPS (△) in an aqueous solution under N_2. The spectrum given by crossed symbols is the absorption spectrum of Na_4PS_4 normalized at 370 nm.

the quenchers investigated were less effective even at the highest concentration.

The molar extinction coefficient for the T−T absorption was determined using the ground state (S0) depletion method. In this experiment, we measured the TA spectra with a very low-energy laser pulse (about 3 mJ/cm^2) in a wide range of wavelengths involving the S0−S1 and S0−S2 transition regions. Therefore, the transients observed within the temporal range investigated could be restricted only to the triplet and the intermediates formed via the one-photon process. In fact, the contributions from the multiphoton processes were found to be negligible on the basis of the quenching experiments with N_2O and O_2.

Under these conditions, the difference between the observed absorbances at wavelength λ before and t μs after laser irradiation, $A_0(\lambda)$ and A(λ,t), respectively, is given by

$$\Delta A(\lambda,t) = A_0(\lambda) - A(\lambda,t)$$
$$= [\epsilon_0(\lambda)(C_0 - C_T(t)) - \epsilon_T(\lambda)C_T(t) - \sum \epsilon_i(\lambda)C_i(t)]L$$

where ϵ_0, ϵ_T, and ϵ_i and C_0, $C_T(t)$, and $C_i(t)$ are the molar extinction coefficients and the concentrations of S0, T, and one-photon intermediate (i), respectively. The effective cell length L was 1.0 cm in this experiment. If we can assume that $\epsilon_T(\lambda)$ and $\epsilon_i(\lambda)$ (or $C_i(t)$) are zero in a specific range of wavelengths, $C_T(t)$ and thus the molar extinction coefficient of the triplet at the T−T absorption maximum (λ_{max}), $\epsilon_T(\lambda_{max})$, are given by

$$C_T(t) = C_0 - \Delta A(\lambda,t)/\epsilon_0(\lambda)$$

$$\epsilon_T(\lambda_{max}) = A_T(\lambda_{max},t)/C_T(t)$$

where $A_T(\lambda_{max},t)$ is the absorbance at λ_{max} due to the T−T absorption.

In Figure 7, the difference spectrum of PS_4^{4-}, presented by the relation between $-\Delta A(\lambda,1\ \mu s)$ and λ, is compared with the absorption spectrum of PS_4^{4-}, normalized at 370 nm. The two spectra were found to agree well in the wavelength region from 355 to 375 nm, of which the deviations were less than 5%. Furthermore, the recovery rates of $A(\lambda,t)$ to $A_0(\lambda)$ were in agreement with the decay rates of the T−T absorption. Thus, the observed decrease in the absorbance was only due to the decrease of concentration of PS_4^{4-} in S0, which was caused by formation of the triplet. In other words, contributions from the triplet and one-photon intermediate in this wavelength region were negligibly small ($\epsilon_T(\lambda) = 0$ and $\epsilon_i(\lambda)$ (or $C_i(t)) = 0$). For PS^-, a similar result was obtained in the wavelength range from 330 to 355 nm. The difference spectrum in Figure 7 also shows that the T−T absorption of PS_4^{4-} had the maximum at 430 nm and several shoulder-like peaks. Those peaks appeared in the TA spectrum observed in aqueous solution containing KI under N_2O in Figure 2B. The difference spectrum of NaPS in Figure 7 also shows three strong peaks at 376, 395, and 420 nm. The former two and the third peak were assigned to those of the intermediate, $(PS^-)^‡$, and T−T absorption, respectively. The values of $A(\lambda,t)$ and $A_T(\lambda_{max},t)$ at $t = 0$ were estimated by fitting the absorbance data to the following bimolecular decay function in the temporal range longer than 0.5−1 μs: $A(t) = A(0)/\{1 + A(0)k_{T-T}t\}$, derived on the basis of the T−T annihilation mechanism. A small but significant contribution of $(PS^-)^‡$ and possibly $(PS_4^{4-})^‡$ to the T−T absorptions at 420 and 430 nm in PS^- and PS_4^{4-}, respectively, could automatically be eliminated by this fitting procedure because those transients decayed within about 1 μs. With the values of $A(\lambda,0)$ at different λ and $A_T(\lambda_{max},0)$ obtained as a function of the concentration C_0 (7×10^{-6} to 4×10^{-5} M), we determined $\epsilon_T(\lambda_{max}/430\ nm)$ for PS_4^{4-} and $\epsilon_T(\lambda_{max}/420\ nm)$ for PS^- to be 17 000 ± 1000 and 23 000 ± 1000 M^{-1} cm^{-1}, respectively. The former value for PS_4^{4-} can be compared with the previously reported value, 19 400 ± 1700 M^{-1} cm^{-1}.[29]

Summary and Outlook for Probing the Micellar Microenvironment

The pyrene derivatives investigated in this study showed different degrees of hydrophilicity. Some of them (PS_4^{4-}, etc.) are highly water-soluble and are expected to exist in the water pool of a reverse micelle. The others, with a weakly hydrophilic substituent such as −COOH (HPB, HPC), are rather water-insoluble in their neutral form. They are likely to locate in the interface region between the water core and the outer oily phase. The TA spectra of these pyrene derivatives in aqueous solution consisted of multiple transients: triplets, cation radicals, anion radicals, hydrated electrons, and the intermediate species produced during photochemical and photophysical processes.

The T−T absorption of the pyrene derivatives appeared at 415−430 nm. The T−T peak of PS_4^{4-} was perturbed little by the other transient species, while the corresponding peaks of PS^-, HPB, and HPC involved a small but significant contribution from the cation radical and the intermediate at high laser power. Their contributions can be evaluated on the basis of the observed dependence on quenchers. The separate spectra, in addition to the molar extinction coefficient of the T−T absorption determined in the present study, will make it possible to quantitatively analyze the decay behavior of T−T absorption and hence elucidate the dynamics of a micellar system in future studies.

The absorption peaks attributable to the cation radicals were observed at 505 nm for polysulfonates (PS_4^{4-} and APS_3^{3-}) and ∼460 nm for monosubstituted pyrenes (PS^-, HPB, and HPC). The cation radicals from the monosubstituted pyrenes were found to exist as a zwitterion. In the absence of any additional quenchers, the cation radicals of the zwitterion-type dominantly decayed via the bimolecular quenching reaction with each parent molecule. This result suggests that the decay rate of an isolated cation radical, for example, generated by ionization of the probe molecule confined in a micelle, would become very slow. These cation radicals were effectively quenched by specific anions such as I^-, OH^-, and SO_3^{2-}, while the other anions such as ClO_4^- and $CH_3SO_3^-$ did not so markedly affect their decay behaviors

even at extremely high concentrations, for example, in 4 M $NaClO_4$ solution. Therefore, it appeared that the highly concentrated ionic environment found in the micellar interface region was not essential for the quenching behavior of the cation radicals generated in a water pool of reverse micelle unless the surfactant molecule itself was an effective quencher.

Acknowledgment. We thank M. Ikeuchi, K. Noguchi, R. Tahara, and M. Hiraoka for their helpful assistance in measurements of TA spectra and analysis of decay kinetics.

Supporting Information Available: Figures 1S showing the dependence of decay curves of the $P^{\bullet+}S^{-}$ cation radical on [NaPS] and comparison with the fitting curves and Figure 2S showing decay behaviors of the cation radical $(PS_4^{4-})^{\bullet+}$ in the presence of $CH_3SO_3^-$, ClO_4^-, and F^- anions. This material is available free of charge via the Internet at http://pubs.acs.org.

References and Notes

(1) Fendler, J. H. *Membrane Mimetic Chemistry*; Wiley Inter-science: New York, 1982; Chapter 2.
(2) Winnik, F. M.; Regismond, S. T. A. *Colloids Surf., A* **1996**, *118*, 1.
(3) Karpovich, D. S.; Blanchard, G. J. *J. Phys. Chem.* **1995**, *99*, 3951.
(4) Kalyanasundaram, K.; Thomas, J. K. *J. Am. Chem. Soc*. **1977**, *99*, 2039.
(5) Zana, R.; In, M.; Lévy, H.; Duportail, G. *Langmuir* **1997**, *13*, 1552.
(6) De, S.; Aswal, V. K.; Goyal, P. S.; Bhatacharya, S. *J. Phys. Chem. B* **1998**, *102*, 6152.
(7) Caldararu, H.; Caragheorgheopol, A.; Vasilescu, M.; Dragutan, H.; Lemmetineu, H. *J. Phys. Chem.* **1994**, *98*, 5320.
(8) Vasilescu, M.; Caragheorgheopol, A.; Caldararu, H.; Bandula, R.; Lemmetineu, H.; Joela, H. *J. Phys. Chem. B* **1998**, *102*, 7740.
(9) Almgren, M.; Wang, K.; Asakawa, T. *Langmuir* **1997**, *13*, 4535.
(10) Ranganathan, R.; Peric, M.; Bales, B. L. *J. Phys. Chem. B* **1998**, *102*, 8436.
(11) Alargova, R. G.; Kochijashky, I. I.; Sierra, M. L.; Zana, R. *Langmuir* **1998**, *14*, 5412.
(12) Correll, G. D.; Chesser, R. N., III; Nome, F.; Fendler, J. H. *J. Am. Chem. Soc*. **1978**, *100*, 1254.
(13) Kalyanasundaram, K. *Photochemistry in Microheterogeneous Systems*; Academic Press: New York, 1991.
(14) Grätzel, M.; Kalyanasundaram, K.; Thomas, J. K. *J. Am. Chem. Soc*. **1974**, *96*, 7869.
(15) Gauduel, Y.; Pommeret, S.; Yamada, N.; Migus, A.; Antonetti, A. *J. Am. Chem. Soc*. **1989**, *111*, 4974.
(16) Mori, Y.; Shinoda, H.; Kitagawa, T. *Chem. Phys. Lett*. **1991**, *183*, 584.
(17) Mori Y.; Shinoda, H.; Kitagawa, T. *Chem. Lett*. **1993**, (1), 49.
(18) Rothenberger, G.; Infelta, P. P.; Grätzel, M. *J. Phys. Chem*. **1981**, *85*, 1850.
(19) Prado, E. A.; Yamaki, S. B.; Atvars, T. D. Z.; Zimerman, O. E.; Weiss, R. G. *J. Phys. Chem. B* **2000**, *104*, 5905.
(20) Hansson, P.; Jönsson, B.; Ström, C.; Söderman, O. *J. Phys. Chem. B* **2000**, *104*, 3496.
(21) Lissi, E. A.; Abuin, E. B.; Rubio, M. A.; Ceron, A. *Langmuir* **2000**, *16*, 178.
(22) Hasegawa, M. *Langmuir* **2001**, *17*, 1426.
(23) Jardon, P.; Lazorchak, N.; Ganton, R. J. *J. Chim. Phys. Phys.-Chim. Biol*. **1986**, *83*, 311.
(24) Palit, D. K.; Pal, H.; Makherjee, T.; Mittal, J. P. *J. Photochem. Photobiol., A: Chem*. **1988**, *43*, 59.
(25) Wenz, M.; Zhang, M.-H.; Wang, Q.-H.; Shen, T. *J. Chem. Soc., Faraday Trans.* **1997**, *93*, 3491.
(26) Hunter, T. F.; Younis, A. I. *J. Chem. Soc., Faraday Trans*. **1979**, *75*, 550.
(27) Yasoshima, S.; Masuhara, H.; Mataga, N.; Suzuki, H.; Uchida, T.; Minami, S. *Bunko Kenkyu* **1981**, *30*, 93.
(28) Yamamoto, I.; Shiraki, S.; Kawamura, Y. *J. Chem. Soc., Perkin Trans. 2* **1992**, 2241.
(29) Bohme, C.; Abuin, E. B.; Scaiano, J. C. *J. Am. Chem. Soc*. **1990**, *112*, 4226.
(30) Koike, K.; Thomas, J. K. *J. Chem. Soc., Faraday Trans*. **1992**, *88*, 195.
(31) Grätzel, M.; Kozak, J. J.; Thomas, J. K. *J. Chem. Phys*. **1975**, *62*, 1632.
(32) Badger, B.; Brocklehurst, B. *Trans. Faraday Soc*. **1969**, *65*, 2588.
(33) Janata, E.; Schuler, R. H. *J. Phys. Chem*. **1982**, *86*, 2078.
(34) Grossweiner, L. I.; Matheson, M. S. *J. Phys. Chem*. **1957**, *61*, 1089.
(35) Richards, J. T.; West, G.; Thomas, J. K. *J. Phys. Chem*. **1970**, *74*, 4237.
(36) Shinoda, H.; Mori, Y.; Kitagawa, T. *J. Mol. Struct. (THEOCHEM)* **2001**, *546*, 195.